Supplementary Data

Image Processing Workflow Diagram

A - Preprocessing

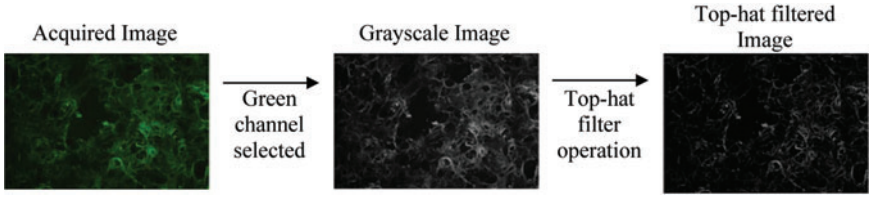

B - Hough Transform

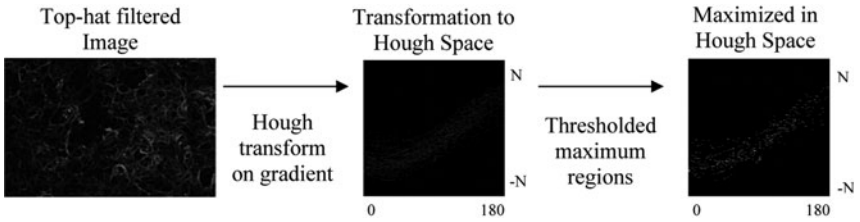

C - Angle Histogram (Rose Plot)

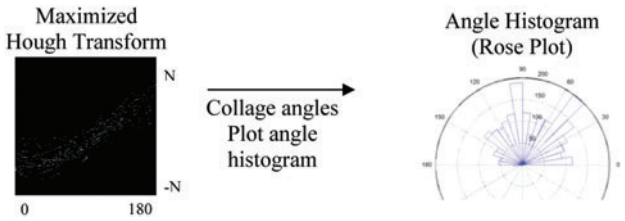

D - Determination of holes

Description of Image Processing Workflow

The key steps to image processing were **(A)** preprocessing, **(B)** Hough space transformation, calculation of the **(C)** directional distribution, and **(D)** hole parameters of the collagen network, shown in the workflow diagram.

In **(A)**, input images of extracelluar matrix deposition were acquired with an IX71 inverted fluorescence microscope (Olympus) with a resolution of 1024 by 1360 pixels. The green channel image was extracted and median-filtered. To enhance the image contrast, we applied morphological top-hat filtering. This top-hat filter used a disk-structuring element function of 12 pixels. With this function, we computed the morphological opening of the image, which was then subtracted from the original image.

To obtain the directional coherence of the collagen structure, we transformed the image to a different domain using the Hough transform, shown in **(B)**. This domain reduced the image to a set of independent directional distributions with regard to the x-axis. Hough transforms are used to analyze features such as straight lines.[1] A line can be specified by its orientation θ, bounded by the angles [0,180°], with regard to

Supplementary Table S1. Primer Sequences (5′→3′, Forward and Reverse)

Gene	*Accession no.*	*Sequence*	*Reference*
RPLP0	NM_001002.3	TGT TGC CAG TGT CTG TCT GC CTC GTT TGT ACC CGT TGA TGA	—
PPAR-γ	NM_015869.4	CAG ACA GAT TGT CAC GGA ACA GGC AGT GGC TCA GGA CTC	—
FABP4	NM_001442.2	TGT GCA GAA ATG GGA TGG AAA CAA CGT CCC TTG GCT TAT GCT	Elabd *et al.*[1]
GLUT4	NM_001042.2	TCA ACA ATG TCC TGG CGG TG TTC TGG ATG ATG TAG AGG TAG CGG	Lee *et. al.*[2]
LEP	NM_000230.2	CCA TCC AGA ATA AAA CGC AAA GGG TCA CCA GTG TGG GAC CGT CA	—
FGF2	NM_002006.4	GAG AAG AGC GAC CCT CAC A TAG CTT TCT GCC CAG GTC C	Li *et al*. 2008[3]

RPLP0, human ribosomal phosphoprotein P0; TBP, TATA-box-binding protein; PPAR-γ, peroxisome proliferator-activated receptor gamma; FABP4, fatty acid-binding protein 4; GLUT4, glucose transporter type 4; LEP, leptin; FGF-2, fibroblast growth factor 2 (basic).

1. Elabd, C., Basillais, A., Beaupied, H., Breuil, V., Wagner, N., Scheideler, M., *et al*. Oxytocin controls differentiation of human mesenchymal stem cells and reverses osteoporosis. Stem Cells **26,** 2399, 2008.

2. Lee, E.K., Lee, M.J., Abdelmohsen, K., Kim, W., Kim, M.M., Srikantan, S., *et al*. miR-130 suppresses adipogenesis by inhibiting peroxisome proliferator-activated receptor gamma expression. Mol Cell Biol **31,** 626, 2011.

3. Li, X., An, H.S., Ellman, M., Phillips, F., Thonar, E.J., Park, D.K., *et al*. Action of fibroblast growth factor-2 on the intervertebral disc. Arthritis Res Ther **10,** R48, 2008.

the x-axis and a distance ρ from the origin. The equation for a line segment is, therefore, $\rho = x\cos\theta + y\sin\theta$ If we convert each point in the image (x_i, y_i), we would obtain an image showing the sinusoidal curve in the Hough domain (ρ, θ). The mapping of points in a line would be a common point of ρ_0 and θ_0 Therefore, the larger linear segments would have larger-valued ρ, θ points in the Hough domain.

The standard Hough transform in MATLAB is applicable to binary images. Therefore, the transform depends on the technique applied to obtain the binary image, such as edge detection or thresholding.[1] The variations (gradients) in intensity correspond to the volume of collagen IV fibers formed. This information is lost from the binary image. We performed a modified of the Hough transform that uses the gradient intensity for a more informative transformation. The higher the gradient in the image, the more defined are the collagen fibers. The gradient ∇F of each point in the image is obtained by combining the gradient in the x and y directions of the image, $\nabla F = \partial F/\partial x\vec{i} + \partial F/\partial y\vec{j}$. We calculated the modified Hough transform by incrementing each ρ, θ point with the gradient, whereas the standard Hough transform increments this point by one. Hence, brighter intensity gradient changes corresponded to brighter peaks in the Hough domain and a higher weighage for directional distribution computation. We

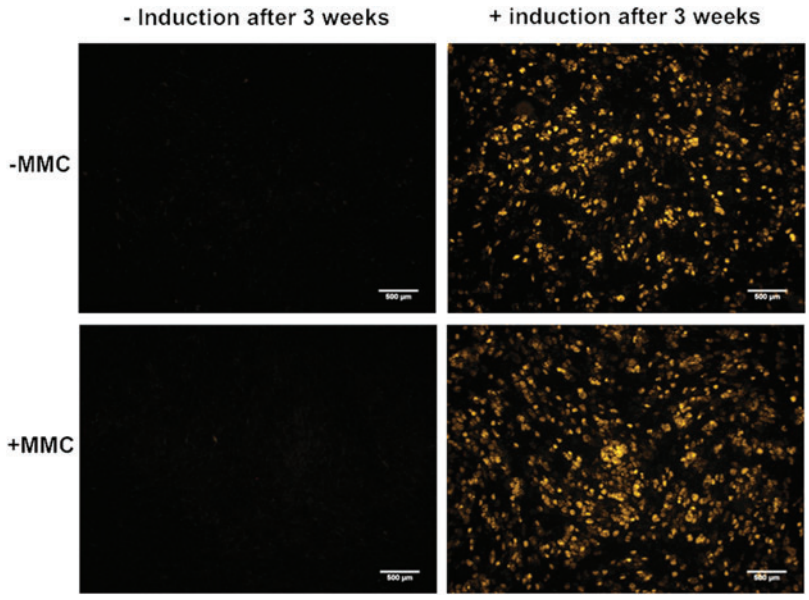

SUPPLEMENTARY FIG. S1. Macromolecular crowding does not spontaneously induce adipogenesis in mesenchymal stem cells (MSCs) after 21 days. MSCs maintained in basal media did not exhibit any signs of differentiation, confirming that the MMC cocktail per se is not inherently adipogenic. (Scale bar: 500 μm).

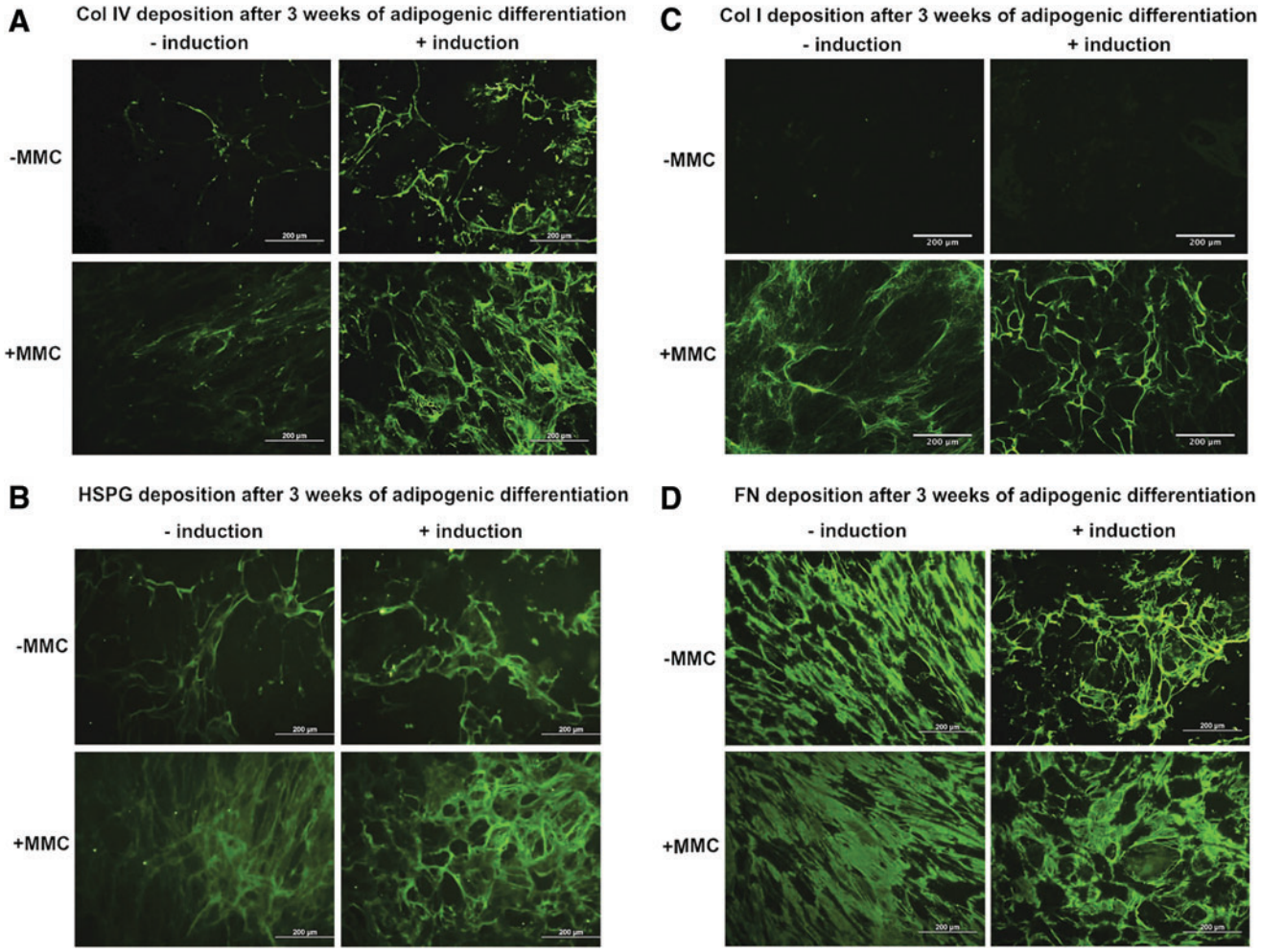

SUPPLEMENTARY FIG. S2. Enhanced remodeling of adipogenic extracellular matrix (ECM) under macromolecular crowding after 21 days of adipogenic differentiation. Representative immunocytochemistry images of **(A)** Col IV, **(B)** HSPG, **(C)** Col I, and **(D)** FN of MSCs that underwent adipogenic differentiation ± MMC compared with nondifferentiated (-induction) controls at 20X magnification. The remodeling from a fibrillar MSC matrix to a recticular adipocyte matrix was more evident under + MMC conditions. Scale bar: 200 μm.

computed the directional distribution by detecting the peaks in the Hough parameter space by intensity thresholding.[2]

Angle histograms (rose plots) enable us to display the directional distribution in a graphical representation **(C)**. The peak angles (θs) from the Hough transforms were sorted into 40 equally spaced bins of angles. The number of angles corresponding to each interval of 9° was represented by a petal of the rose, plotted with its apex at the origin. The more elements within each angle bin, the larger the petal size.

Another metric that is used to quantify the geometric changes in collagen is the number of holes formed **(D)**. We first obtained a binary image via intensity thresholding[2] of the top-hat filtered image from **(A)**. Next, the connected thresholded pixels were clustered into separate objects. The exterior boundaries (shown in red) and holes were traced.[3] We defined the range of holes in the collagen network to have an average diameter between 26 and 300 μm. Traced holes with an average diameter fewer or exceeding this range were removed. The extracted holes (within the desired range) are shown in green.

Supplementary References

1. Rangayyan, R.M., and Rolston, W.A., Directional image analysis with the Hough and Radon transforms. J Indian Inst Sci **78,** 17, 1998.
2. Otsu, N. A Threshold selection method from gray-level histograms. IEEE Trans Syst Man Cybernet **9,** 62, 1979.
3. Gonzalez, R.C., Woods, R.E., and Eddins, S.L. Digital Image Processing Using MATLAB. New Jersey, Pearson Prentice Hall, 2004.

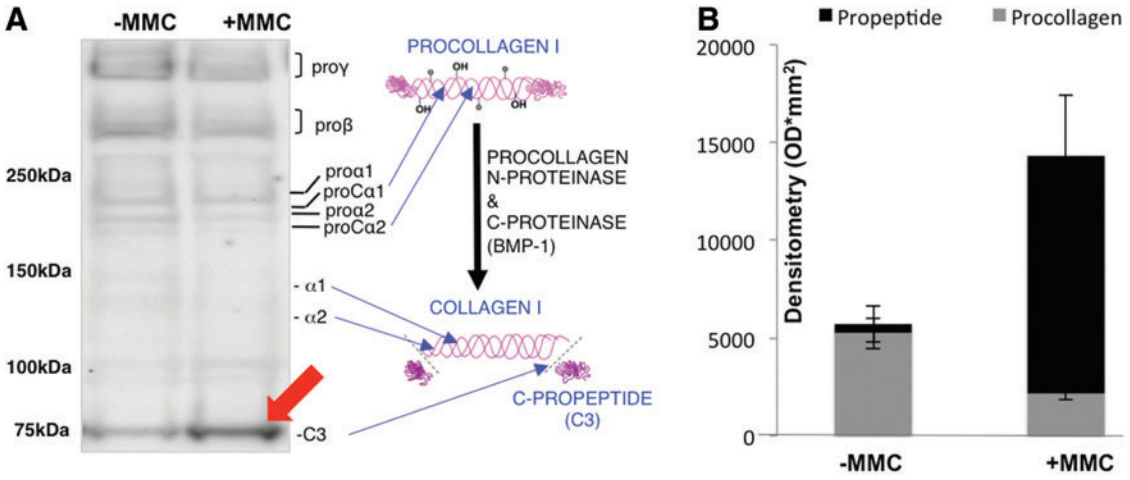

SUPPLEMENTARY FIG. S3. Macromolecular crowding enhances the proteolytic processing of pro-collagen I to collagen during the early stage of adipogenic differentiation of MSCs. **(A)** Immunoblot for cleaved pro-collagen I C-propeptide, 75kDa (C3; red arrow) in medium extracted from adipogenically induced MSCs after 4 days in culture. Under +MMC, more procollagen I was trimmed to collagen I as evident from the simultaneous decrease of procollagen bands and an increase of free C3 in culture media. **(B)** Densitometry analysis of the immunoblot indicates a 25-fold increase of C3 (black bar).

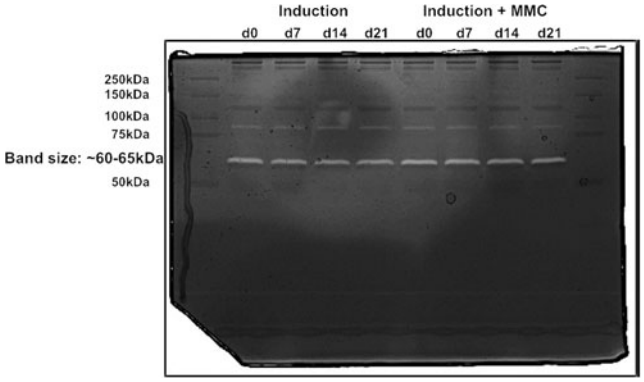

SUPPLEMENTARY FIG. S4. Harvested media of MSCs undergoing adipogenic differentiation show no difference in matrix metalloproteinases (MMP) amounts. Gelatin zymography was performed on media harvested from MSCs undergoing adipogenic induction at the various time points to assess active MMP activity. There was no difference in the amounts of MMP between induction and induction +MMC samples at each time point.

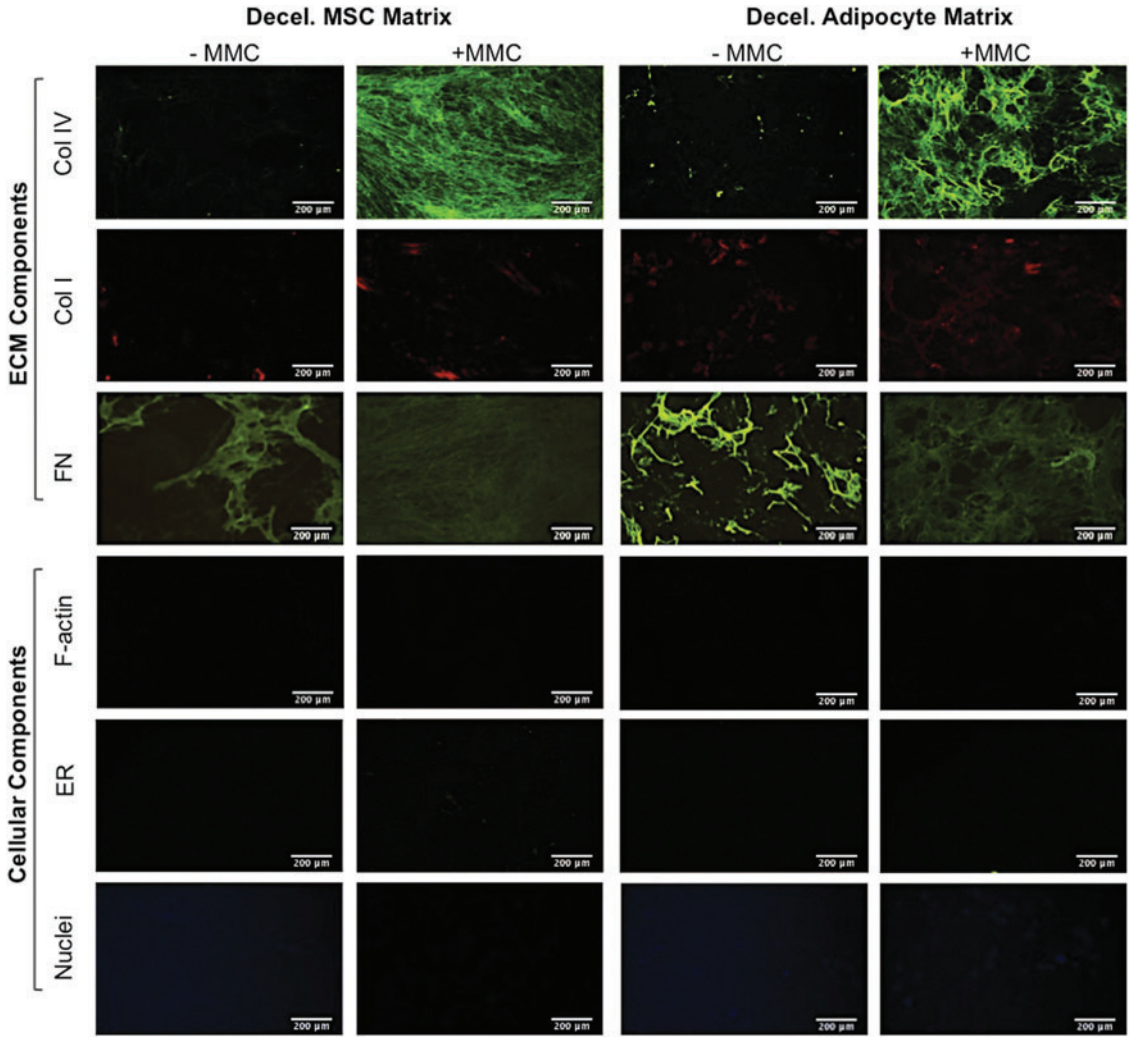

SUPPLEMENTARY FIG. S5. Decellularized matrices retain their matrix components but not cellular components. Decellularized matrices retained their matrix components, especially for the matrices generated under +MMC but not cellular components. Scale bar: 200 µm.

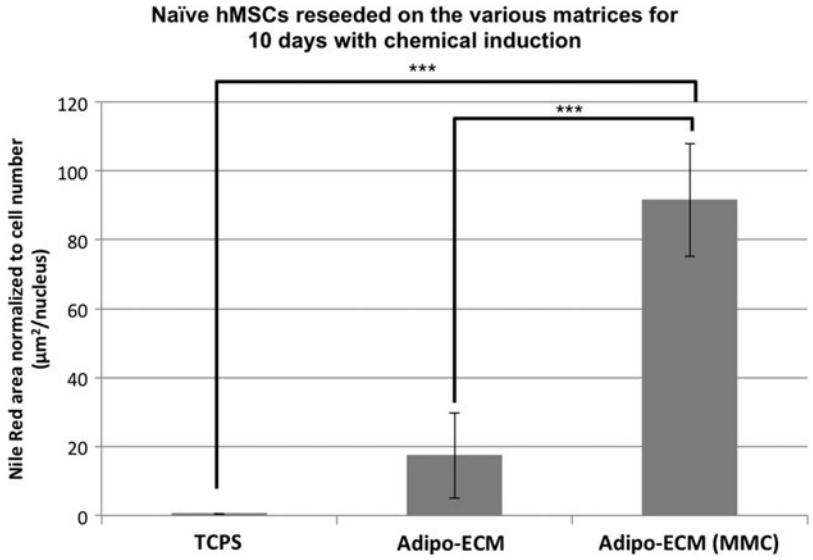

SUPPLEMENTARY FIG. S6. MSCs differentiated on Adipo-ECM (+MMC) accumulated substantial lipid already after 10 days of induction. MSCs differentiated on Adipo-ECM (+MMC) adipocyte matrices generated under MMC showed a five-fold increase in Nile Red fluorescence area per cell compared with those differentiated on Adipo-ECM alone, demonstrating accelerated adipogenesis at 10 days. Compare with Figure 7. $^{*}p < 0.05$, $^{**}p < 0.01$ and $^{***}p < 0.001$.

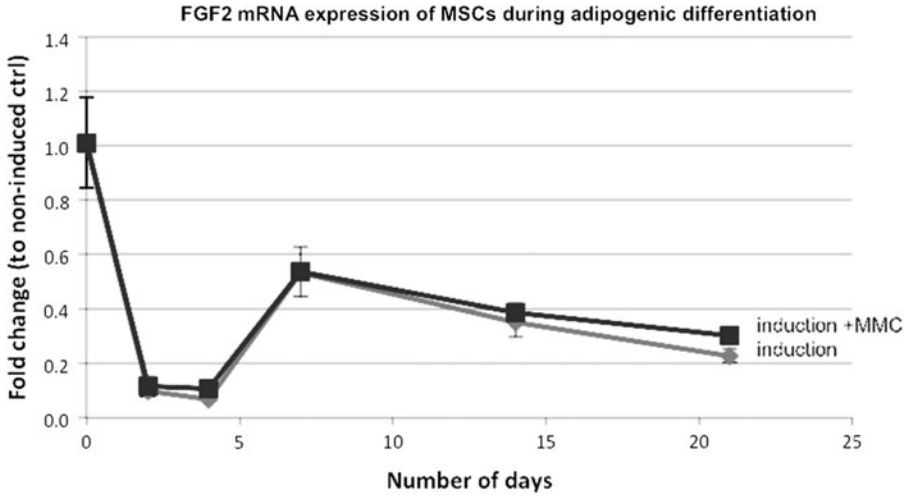

SUPPLEMENTARY FIG. S7. Cellular mRNA expression of FGF2 by MSCs during adipogenic differentiation. MSCs express high levels of FGF2 expression at the start of differentiation.